



Growth of titanium oxynitride layers by short pulsed Nd:YAG laser treatment of Ti plates: Influence of the cumulated laser fluence

L. Lavissee^{a,*}, M.C. Sahour^a, J.M. Jouvard^a, G. Pillon^a, M.C. Marco de Lucas^b, S. Bourgeois^b, D. Grevey^a

^a Institut Carnot de Bourgogne, UMR 5209 CNRS-Université de Bourgogne, 12 Rue de la Fonderie, F-71200 Le Creusot Cedex, France

^b Institut Carnot de Bourgogne, UMR 5209 CNRS-Université de Bourgogne, 9 Av. A. Savary, BP 47 870, F-21078 Dijon Cedex, France

ARTICLE INFO

Article history:

Available online 9 August 2008

Keywords:

Titanium oxycarbides
Titanium oxynitrides
Laser treatment
Plasma

ABSTRACT

Titanium oxynitride layers were formed by surface laser treatment of Ti plates in air using a Nd:YAG laser source of short pulse duration about 5 ns. The cumulated laser fluence was varied in the 100–1200 J cm⁻² range and its influence on the composition and the structure of the formed layers was studied by different characterization techniques providing physico-chemical and structural information. It was shown that the laser treatment induces the insertion of light elements as O, N and C in the formed layer with the amount increasing with the laser fluence. The in-depth composition of the layers and the co-existence of different phases were also studied.

The way in which the laser parameters such as fluence affect the insertion of nitrogen and oxygen was discussed in connection with the effects of the plasma plume formed above the target.

© 2008 Elsevier B.V. All rights reserved.

1. Introduction

From an applicative point of view it is of particular interest to obtain in a simple process titanium oxynitrides, TiN_xO_y, mixed phases which can combine the stability of titanium oxides and the hardness of titanium nitride TiN. Many procedures have been carried out for producing titanium oxynitrides in a controlled atmosphere [1–3].

The surface of titanium targets can be modified by a variety of laser treatments carried out in air. Different compounds are likely to be formed: oxides, which may be used for tribological purposes [4] or for colouring [5], and nitrides, for their hardening properties [6–8].

From a fundamental point of view, it is also of interest to get information on laser induced insertion phenomena.

It is from this perspective that surface laser treatments were carried out on titanium substrates in ambient air to obtain layers of titanium oxynitrides by using a Nd:YAG laser source with a pulse duration of about 5 ns.

In this work, we analyse the influence of the cumulated laser fluence on the composition and the structure of the obtained layers. Results are obtained by means of scanning electron microscopy (SEM), X-ray microanalysis (energy dispersive spectro-

metry, EDS) and X-ray diffraction (XRD) with different incidence angles for the in-depth study of the layers. The layer properties are discussed as a function of the laser treatment conditions.

2. Experimental details

2.1. Substrates

Commercially pure (CP) titanium substrate (grade 4) samples were used. Before laser treatment, the sample surfaces (20 mm × 15 mm × 15 mm) were mechanically polished to obtain a reference surface with roughness less than 0.4 μm.

2.2. Laser treatments

The laser treatments were performed in air using a Nd:YAG Q-switched laser (Quantel Brillant B model) with a 1.064 μm wavelength, which generates pulses of 5 ns duration at a repetition rate of $f = 10$ Hz. The focused laser spot, with a diameter of about 1.6 mm and a Gaussian energy distribution, was moved over the substrate surface to form parallel straight lines with a velocity, v , going from 100 to 165 mm s⁻¹. The distance, d , between adjacent lines was varied from 0.15 to 0.27 mm. By varying the mean laser fluence per pulse, F_{ip} , and the number of impacts, n_p , layers of various colours were formed on the target surface. The cumulated laser fluence, F_l (in J cm⁻²), corresponding to the total energy per surface unit can be calculated by the equation: $F_l = F_{ip} \times n_p$.

* Corresponding author. Tel.: +33 3 85 42 43 19; fax: +33 385 424 466.

E-mail address: luc.lavissee@u-bourgogne.fr (L. Lavissee).

2.3. Characterization techniques

Surface and cross-sectional observations were carried out using a SEM microscope equipped with an EDS microprobe (EDS – OXFORD – Inca energy software). The apparatus was a JEOL JSM 6400F that functions typically at 20 keV. Cu ($K_{\alpha 1}$) radiation was used for small angle incidence XRD experiments. The incidence angle θ was varied in the $0.5\text{--}8^\circ$ range in order to analyse the samples at different depths going from about $0.2\ \mu\text{m}$ for $\theta = 0.5^\circ$ to about $3\ \mu\text{m}$ for $\theta = 8^\circ$.

3. Results and discussion

3.1. Laser substrate interaction: thermal modelling

By varying the cumulated laser fluence layers of various colours were formed on the target surface. Table 1 summarizes the laser treatment conditions used in this work as well as the properties of the corresponding layers.

Intense vaporisation of the target is to be expected with values of the laser irradiance per pulse higher than $10^{12}\ \text{W m}^{-2}$ and pulse duration of about 5 ns [9]. A thermal simulation was carried out using COMSOL MULTIPHYSICS code. This simulation shows that the surface reaches vaporisation temperature very quickly and tends towards the limit indicated by Semak in his model [10]. An arbitrary Lagrange Euler method for a 2D axisymmetric model was used [11] to take into account the motion of the molten metal, pushed back on the edge of the laser interaction zone under recoil pressure action. We associate the thermal equations, fluids and surface tension. The recoil pressure and the energy loss through vaporisation were calculated using the Semak model. The estimates from these models are the following:

- The layer of liquid metal is very thin, from about $0.1\ \mu\text{m}$ to some tenths of micrometers, which is consistent with Schaaf works [12].
- The recoil pressure is above $10^9\ \text{Pa}$.
- The molten metal is pushed back on the sides of the impact [13]. The ejection speed is around $600\ \text{m s}^{-1}$.

It can be supposed that at the end of the pulse almost all the energy has been involved in the vaporisation of the target surface.

Table 1

Laser treatment conditions and properties of the different layers analysed in this work

	Samples			
	S1	S2	S3	S4
Laser treatment conditions				
d (mm)	0.27	0.21	0.18	0.15
ν (mm s ⁻¹)	164	132	105	97
P_1 (W)	0.84	1.9	1.54	2.92
n_p	28	44	68	83
F_{1p} (J cm ⁻²)	4.2	9.5	7.7	14.5
I_{1p} ($\times 10^{12}$ W cm ⁻²)	8.4	19.0	15.3	8.4
F_1 (J cm ⁻²)	120	420	520	1200
Sample properties				
Colour	Yellow	Purple	Blue	Green
N + O (at.%)	32	61	63	65
N (at.%)	12	18	20	13
Lattice parameter, a (nm)	0.420	0.423	0.422	0.424

d is the distance between adjacent scanning lines, ν the laser velocity on the target, P_1 the average laser power, n_p the number of impacts per point, F_{1p} the fluence per pulse, I_{1p} the laser irradiance per pulse, and F_1 is the cumulate fluence. The elementary composition was determined by EDS analysis and the lattice parameter, a , was calculated from the position of the (2 0 0) peak assigned to a fcc phase in the XRD diffraction patterns obtained with an incidence angle of 8° .

Then, the ratio between the power of the laser beam absorbed by the plume above the target and that directly absorbed by the target is higher than the unity: the plume absorbs more than the neutral gas. The layer of material removed by ablation is about $1\ \mu\text{m}$ thick.

3.2. Morphology and composition of the layers

The existence of a thin molten pool during the laser treatment is confirmed by the SEM observations of the layers surface (Fig. 1) showing projections lengthened by droplets and some cracks. The laser treatment conditions used in this work (Table 1) lead to small quantities of ejected material around the treated zones. Cross-sectional observations show that the depth affected by the laser treatment is about $2\ \mu\text{m}$.

The results of the EDS analyses carried out on the top of the laser treated samples are summarized in Table 1. It is worth noting the high amount of nitrogen and oxygen in the layers, which increases with the cumulated laser fluence mainly in the $100\text{--}400\ \text{J cm}^{-2}$ range where the nitrogen plus oxygen content increases from about 30 at.% to about 60 at.%. For higher laser fluence values, the content in N and O slightly increases, up to about 65 at.% for a laser fluence of $1200\ \text{J cm}^{-2}$. Besides, the insertion of nitrogen and oxygen seems to vary in a different way as a function of the laser fluence. The nitrogen content increases up to about 20 at.% for $F_1 = 520\ \text{J cm}^{-2}$ and slightly decreases for higher F_1 values. On the other hand, the oxygen content increases by a factor 2 in the $100\text{--}400\ \text{J cm}^{-2}$ range, is almost constant up to $500\ \text{J cm}^{-2}$ and slightly increases for higher F_1 values. This different behaviour has been dealt with in an earlier study [14].

The EDS analysis of cross-sections shows that there is no more nitrogen or oxygen about $3\ \mu\text{m}$ below the surface.

3.3. XRD results

Fig. 2 shows the XRD patterns obtained with an incidence angle of 8° for the samples summarized in Table 1. The four patterns display similar diffraction peaks, but it is worth noting that some peaks display a significant shift to lower diffraction angles by increasing the laser fluence.

The diffraction lines corresponding to the Ti substrate are observed only for incidence angles higher than 5° , that is to say for a probe depth of about $3\ \mu\text{m}$, which agrees with the EDS results.

The diffraction peaks can be assigned to two kinds of phases:

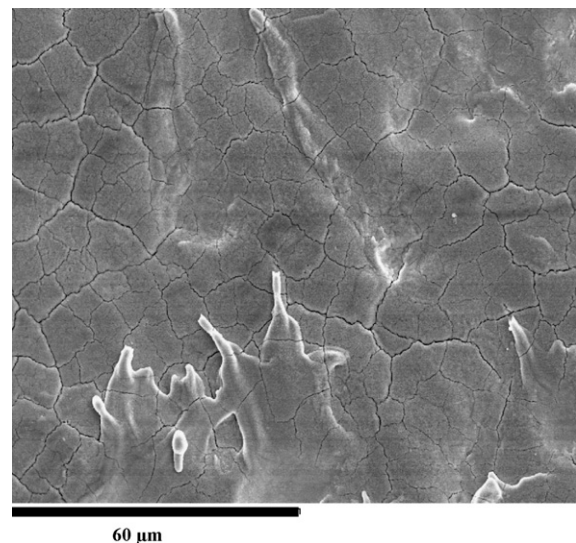


Fig. 1. SEM top view of sample S3 obtained with a laser fluence $F_1 = 520\ \text{J cm}^{-2}$.

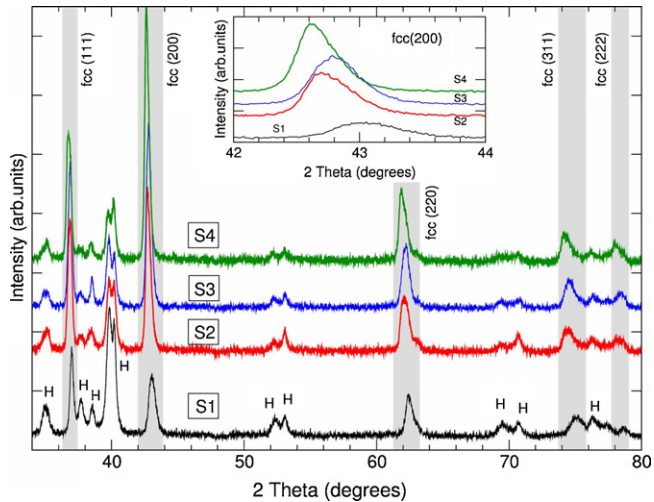


Fig. 2. XRD patterns of the samples S1 to S4 obtained with increasing laser fluence values indicated in Table 1. The incidence angle was equal to 8° . H denotes peaks corresponding to a hexagonal phases. The diffraction peaks assigned to a fcc phase are indicated by grey bands. The inset displays a magnification of the patterns in the region of the fcc(2 0 0) peak.

- Phases with hexagonal symmetry, corresponding to the peaks labelled H in Fig. 2. These peaks appear at almost the same position for all the samples. Besides the substrate, two insertion phases were identified: Ti_3O (fiche JCPDS 76-1644) and $\text{TiN}_{0.3}$ (fiche JCPDS 41-1352).
- Phases with cubic symmetry (face centered cubic phases), corresponding to the diffraction peaks exhibiting a shift as a function of the laser fluence. Titanium nitride TiN (JCPDS 38-1420) and titanium monoxide $\text{TiO}_{1.04}$ (JCPDS 43-1296) display stable phases at high temperature [15–17] with diffraction peaks in good agreement with those labelled fcc in Fig. 2. This supports the fact that in the layers, titanium oxynitride Ti_xO_y phases with fcc structure grow in our experimental conditions [1,2,18,19]. The lattice parameter determined from the position of the (2 0 0) peak (Table 1) increases from 0.420 nm for the sample S1 up to 0.424 nm for the sample S4, which agrees with the lattice parameter of TiN [20].

In-depth structural analyses of the layers were done by varying the X-ray incidence angle in the $0.5\text{--}8^\circ$ range. Fig. 3 displays the patterns obtained for the sample S4 in the region of the (2 0 0) peak as a function of the incidence angle. The decrease of the incidence angle from 8° to 5° induces a very small shift of the (2 0 0) peak, but for lower incidence angles the peak position significantly shifts to lower diffraction angles and it becomes near the position of the (2 0 0) peak in titanium carbonitrides $\text{TiN}_{0.3}\text{C}_{0.7}$ (JCPDS 42-1489), oxycarbides $\text{Ti}(\text{C}, \text{O})$ [21] and carbide TiC (JCPDS 31-1400).

4. Discussion

XRD results could be explained by a gradient in the quantity of light elements in the layer and a higher level of carbon insertion near the surface layer. As an earlier study has already shown [22], there is carbon on the extreme surface of a layer produced by a laser source Nd:YAG with a longer pulse duration. These carbides may be formed from the high reactivity of the elements in the plasma [23,24] or in the liquid [25]. Since the energy from the laser source serves essentially to heat the metallic vapours, a reduction in the duration of the pulse favours the phenomena related to plasma at the expense of those related to a liquid bath like diffusion

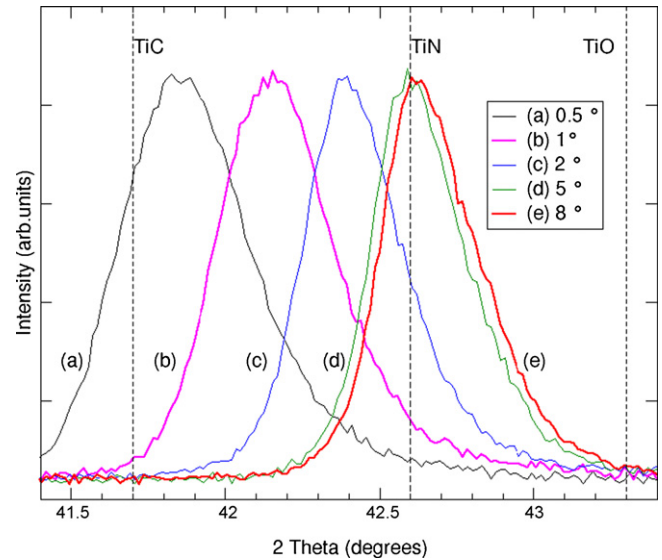


Fig. 3. (a–e) XRD patterns obtained with different X-ray incidence angles, going from 0.5° to 8° , for the sample S4 ($F_1 = 1200 \text{ J cm}^{-2}$) in the range of the (2 0 0) diffraction peak assigned to a fcc phase. Vertical lines indicate the position of the (2 0 0) peak for TiO, TiN and TiC.

[12]. The phases observed on the extreme surface of the layers are thus formed during the final impact, since the thickness removed by ablation is greater than that of the liquid. It is not the accumulation of the laser impacts that produces this thickness, for that would lead to a high level of insertion of light elements (nitrogen and oxygen).

No evidence of titanium dioxide phases was found, even though the laser fluence values used in this work induced the growth of titanium dioxide layers in previous works where longer pulse durations about 35 ns were used [22,26]. In fact, the pulse duration is an important factor in the reactivity of the plasma. Höche et al. [27] showed for an infrared source at $3.13 \mu\text{m}$ with a very short pulse duration, about 0.1 ps, that the plasma formed above the target dissociates the nitrogen molecules N_2 . In our study, the energy conditions for the plasma are such that the nitrogen molecules are at least partially dissociated [9]. For laser pulse duration of some nanoseconds, layers of titanium oxynitrides are obtained with a variable in-depth content of nitrogen and oxygen in the layer. This effect is not found for longer pulse durations ($\sim 35 \text{ ns}$) [5,12,26].

5. Conclusion

A pulsed laser beam Nd:YAG emitting at $1.064 \mu\text{m}$ with pulse duration of about 5 ns was used for the laser treatment of commercially pure titanium targets. In these conditions, a thin liquid zone about 100 nm thick has been formed at the surface target with an intense vaporization which induces a plume under the target. This laser treatment induced the insertion of light elements, nitrogen and oxygen, in the target leading to the growth of titanium oxynitrides layers with a thickness of about $2 \mu\text{m}$. The influence of the cumulated laser fluence on the properties of the layer was studied in the $100\text{--}1200 \text{ J cm}^{-2}$ range. EDS analysis showed that the oxygen and nitrogen content increases with the cumulated laser fluence, though the nitrogen content stabilizes around 20 at.% for a laser fluence about 400 J cm^{-2} .

X-ray diffraction experiments with different incidence angles were done for the in-depth study of the layers. The phases of inserted Ti_nX (N and O) with a hexagonal symmetry were found immediately above the Ti substrate, but the layers were mainly

composed of titanium oxynitrides TiN_xO_y displaying a fcc phase. Near the layer surface a very thin layer of titanium oxynitrocarbides $Ti(C, N, O)$ could be formed.

The reactivity of the different chemical species present in the plasma formed above the target is of great importance for the understanding the composition and properties of the layers. Work is in progress to analyse the composition of the plasma plume (ionisation rate, concentration of species), as well as the influence of this plume on the interaction.

Acknowledgements

We would like to thank C. Josse (ICB) for SEM experiments and A. Tidu (LETAM) for discussions on titanium oxynitrides and carbonitrides. This work has been financially supported by the Conseil Regional de Bourgogne.

References

- [1] M. Braic, M. Balaceanu, A. Vladescu, A. Kiss, V. Braic, G. Epurescu, G. Dinescu, A. Moldovan, R. Birjega, M. Dinescu, *Appl. Surf. Sci.* 253 (2007) 8210.
- [2] F. Vaz, P. Cerqueira, L. Rebouta, S.M.C. Nascimento, E. Alves, Ph. Goudeau, J.P. Riviere, K. Pischow, J. de Rijk, *Thin Solid Films* 447–448 (2004) 449.
- [3] J. Guillot, F. Fabreguette, L. Imhoff, O. Heintz, M.C. Marco de Lucas, M. Sacilotti, B. Domenichini, S. Bourgeois, *Appl. Surf. Sci.* 177 (2001) 268.
- [4] C. Langlade, A.B. Vannes, J.M. Krafft, J.R. Martin, *Surf. Coat. Technol.* 100–101 (1998) 383.
- [5] A. Perez del Pino, P. Serra, J.L. Morenza, *Thin Solid Films* 415 (2002) 201.
- [6] A.L. Thomann, E. Sicard, C. Boulmer-Leborgne, C. Vivien, J. Hermann, C. Andreazza-Vignolle, P. Andreazza, C. Meneau, *Surf. Coat. Technol.* 97 (1997) 448.
- [7] E. György, A. Perez del Pino, P. Serra, J.L. Morenza, *Appl. Surf. Sci.* 186 (2002) 130.
- [8] D. Höche, G. Rapin, J. Kaspar, M. Shinn, P. Schaaf, *Appl. Surf. Sci.* 253 (2007) 8041.
- [9] D. Bauerle, *Laser Processing and Chemistry*, 2nd ed., Springer, Berlin, 1996, p. 6.
- [10] V. Semak, A. Matsunawa, *J. Phys. D: Appl. Phys.* 30 (1997) 2541.
- [11] A. Soveja, J.M. Jouvard, D. Grevey, in: *Proceedings of European COMSOL Conference 2007*, Grenoble, France, October 23–24, 2007.
- [12] P. Schaaf, M. Han, K.-P. Lieb, E. Carpene, *Appl. Phys. Lett.* 80 (2002) 1091.
- [13] C. Illner, P. Schaaf, K.-P. Lieb, *J. Appl. Phys.* 83 (1998) 2907.
- [14] L. Lavissee, J.M. Jouvard, J.P. Gallien, P. Berger, D. Grevey, *Ph. Naudy, Appl. Surf. Sci.* 254 (2007) 916.
- [15] P. Waldner, *Calphad* 23 (2) (1999) 189.
- [16] H.A. Wriedt, J.L. Murray, *J. Alloys Compd.* 8 (1987) 383.
- [17] W.-E. Wang, *J. Alloys Compd.* 233 (1996) 89.
- [18] F. Borgioli, E. Galvanetto, F.P. Galliano, T. Bacci, *Surf. Coat. Technol.* 141 (2001) 103.
- [19] F. Fabreguette, J. Guillot, L.P. Cardoso, R. Marcon, L. Imhoff, M.C. Marco de Lucas, P. Sibillot, S. Bourgeois, P. Dufour, M. Sacilotti, *Thin Solid Films* 400 (2001) 125.
- [20] F. Fabreguette, L. Imhoff, J. Guillot, B. Domenichini, M.C. Marco de Lucas, P. Sibillot, S. Bourgeois, M. Sacilotti, *Surf. Coat. Technol.* 125 (2000) 396.
- [21] W.B. Pearson, *Handbook of Lattice Spacings and Structures of Metals and Alloys*, Pergamon Press, London, 1958.
- [22] L. Lavissee, J.M. Jouvard, L. Imhoff, O. Heintz, J. Korntheuer, C. Langlade, S. Bourgeois, M.C. Marco de Lucas, *Appl. Surf. Sci.* 253 (2007) 8226.
- [23] G. Leggieri, A. Luches, A. Perrone, *J. Vac. Sci. Technol.* 46 (1995) 991.
- [24] J.M. Lackner, W. Waldhauser, R. Ebner, *Surf. Coat. Technol.* 188–189 (2004) 519.
- [25] Y.L. Yang, D. Zhang, H.S. Kou, *Acta. Metall. Sin. (Engl. Lett.)* 20 (2007) 210.
- [26] L. Lavissee, D. Grevey, C. Langlade, A.B. Vannes, *Appl. Surf. Sci.* 186 (2002) 150.
- [27] D. Höche, G. Rapin, P. Schaaf, *Appl. Surf. Sci.* 254 (2007) 888.